

Flame Retardancy and Mechanical properties of EVA Nanocomposites Based on Magnesium Hydroxide Nanoparticles/Microcapsulated Red Phosphorus

Jian-ping Lv, Wen-hong Liu

School of Chemical Engineering, Hefei University of Technology, Hefei, Anhui 230009, People's Republic of China

Received 7 May 2006; accepted 20 November 2006

DOI 10.1002/app.26028

Published online 13 March 2007 in Wiley InterScience (www.interscience.wiley.com).

ABSTRACT: The flame retardancy and mechanical properties of ethylene vinyl acetate (EVA) polymer nanocomposite based on magnesium hydroxide (MH) nanoparticles with lamellar-shape morphological structures and synergistic agent microcapsulated red phosphorus (MRP) have been studied by limiting oxygen index (LOI), cone calorimeter test (CCT), UL-94 test, tensile strength (TS), and elongation at break (EB). Results showed that LOI values of lamellar-like nanosized MH ($50 \times 350 \text{ nm}^2$) samples were 1–7 vol. % higher than those of the common micrometer grade MH (1–2 μm) in all additive levels. When 1–3 phr MRP substituted for nanosized MH filler, LOI value increased greatly from original 37 to 55, and met the V-0 rating in the UL-94 test. The values of TS for MH nanoparticles composites increased from 10.4 to 17.0 MPa as addi-

tive loading levels increased from 80 to 150 phr, respectively, while the corresponding values for common micrometer MH composites decreased steadily from 9.7 to 7.1 MPa. Thermogravimetric analysis (TGA) and dynamic Fourier-transform infrared spectroscopy (FTIR) results revealed two-step flame-retardant mechanism. First, MH particles decompose endothermically with the release of 30.1% hydration water in the 320–370°C temperature range. Second, MRP promote the formation of compact charred layers slowly in the condensed phase in the 450–550°C temperature range. © 2007 Wiley Periodicals, Inc. *J Appl Polym Sci* 105: 333–340, 2007

Key words: flame retardance; mechanical properties; nanocomposites; reinforcement; magnesium hydroxide

INTRODUCTION

In recent years, halogen-free, low smoke, and fume flame-retardant composites are becoming of increasing importance, particularly for polyolefins such as ethylene vinyl acetate (EVA) copolymer used in cable and wire industry, because the halogen-type flame retardant can cause some problems, such as toxicity, corrosion, and smoke.^{1–5} That has promoted the development of halogen-free flame-retardant (HFFR) materials. Many research results showed that magnesium hydroxide (MH) is a nontoxic and smoke-suppressing HFFR additive with high decomposition temperature in flame-retardant (FR) polymeric materials. However, MH has an essential disadvantage that more than 150 phr MH loading is required to meet FR properties, which could be detrimental to the mechanical properties.^{6–8} Although there are articles concerning solving the problem through surface treatment of MH filler such as coating and coupling,^{9–11} the enhancement is limited that the composites are still far away from their applications required good mechanical properties.

Polymer nanocomposites based on EVA/MH/MRP blends can be considered as one of the effective methods for enhancing polymer properties, because of the nanoscale mechanical and FR reinforcement.

Nanocomposites are a combination of two or more phases containing different composites, where at least one of the phases is in the nanoscale regime. These materials exhibit behavior different from conventional composite materials with microscale structure, due to the small size of the structural unit and the high surface-to-volume ratio.

As for MH nanocrystal phase, the morphological structures may also influence its FR effectiveness and the physical properties of polymeric blends. It has been reported that MH nanocrystals may be synthesized with four different morphological structures, which are needle-like, lamellar-like, rod-like, and sand rose, respectively.^{12,13} Among these four different morphological structures, MH nanocrystals with lamellar-shape could preserve higher FR and mechanical reinforcing functions in polymeric composite materials than do other three morphologies, due to the large anisotropy and the overlap tendency of plate-like morphology in polymeric matrix. In addition, small amount of common micrograde microcapsulated red phosphorus (MRP) incorporated in the nanocomposites could produce significant FR

Correspondence to: J.-P. Lv (lvjp@ustc.edu).

synergistic effect with MH nanoparticles. As a result, the physical property of polymeric materials could be improved evidently, and the total loading level of MH filler decreases to some extent. In our previous work, EVA/MH nanocomposites based on lamellar-like MH nanoparticles with 50 nm in diameter and 10 nm in thickness were explored. The results showed that both FR and mechanical properties for lamellar-like MH nanoparticle filler were indeed improved.¹⁴ But it is very difficult to disperse such small size fillers to polymer matrix to achieve higher extent of nanocomposites formation with common blending equipment, because of high melt viscosity and shear stress. A proper increase in lamellar-like MH nanoparticle diameter but keeping at least one dimension, for example thickness in the case, <100 nm could overcome the difficulty in thermal blending, while keeping its inherent nanoscale reinforcement in FR and mechanical properties at the same time.

This work is mainly devoted to report the investigation of FR and mechanical properties of EVA/MH/MRP nanocomposites based on lamellar-like MH nanoparticles with 350 nm in diameter and 50 nm in thickness, which may have practical application in HFFR cable insulation materials. Cone calorimeter test (CCT), thermogravimetric analysis (TGA), limiting oxygen index (LOI) and UL-94 test were used to investigate flame retardancy, and tensile strength (TS) and elongation at break (EB) were used to investigate mechanical properties. FR mechanism of EVA/MH/MRP polymeric blends was also studied by means of dynamic Fourier-transform infrared spectroscopy (FTIR) and TGA.

EXPERIMENTAL

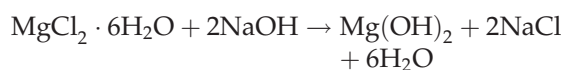
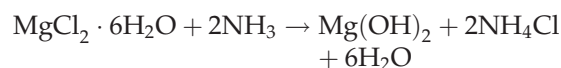
Materials and ingredients

EVA copolymer (containing 28 wt % vinyl acetate) was purchased from Sumitomo Chemical. MRP was prepared in our laboratory, containing 85 wt % P with a particle size range of 1–5 μm . Lamellar-like MH nanoparticles with 350 nm diameter and 50 nm thickness and with a specific surface area of 42 m^2/g were prepared in our laboratory. Micrometer grade MH sample with a specific surface area of 11 m^2/g and particle size range 1–5 μm was obtained from ShanDong Flame Retardant Company (China).

Preparation and characterization of lamellar-like MH nanoparticles

MH nanoparticles were synthesized by a solution chemical process at the presence of complex water-soluble polymer dispersants, which were used to control the morphology of the particles and prevent

the obtained nanocrystals from aggregating. The reaction formulas are given as the follows:



The fabrication of lamellar-like MH nanocrystals can be described as follows. First, 50 g of 50 wt % magnesium chloride hexahydrate aqueous solution and 8 g of 10 wt % complex dispersants aqueous solution of gelatin and lauryl sodium sulfate in the weight ratio of 1 : 1 were put into a 250-mL three-necked flask. Second, 20 g of 25 wt % ammonia water solution was injected into the flask for 1 h, and then 58 g of 8 wt % sodium hydroxide aqueous solution in 2 h was added using a peristaltic pump, under vigorous stirring at 20°C. The mixture was continuously stirred for 1 h, and then transferred to another vessel for hydrothermal treatment at 160°C for 10 h before cooled to room temperature. The resultant suspension was filtered, washed with water to remove the residual impurities. The final product was dried for 24 h at 80°C, yielding a white lamellar-like MH powder (7.2 g, 98% yield based on magnesium chloride hexahydrate).

Figure 1 shows the XRD patterns (2 θ ; scan) of MH nanoparticles synthesized. All the peaks can be indexed to hexagonal MH crystals with lattice constants comparable with the values of JCPDS 7-239. There are no parasite peaks in the XRD patterns of Figure 1, which indicates that MH nanoparticles obtained are relatively pure. Figure 2 shows the field emission scanning electron microanalyser (FESEM) micrographs of the MH particles. The crystals were

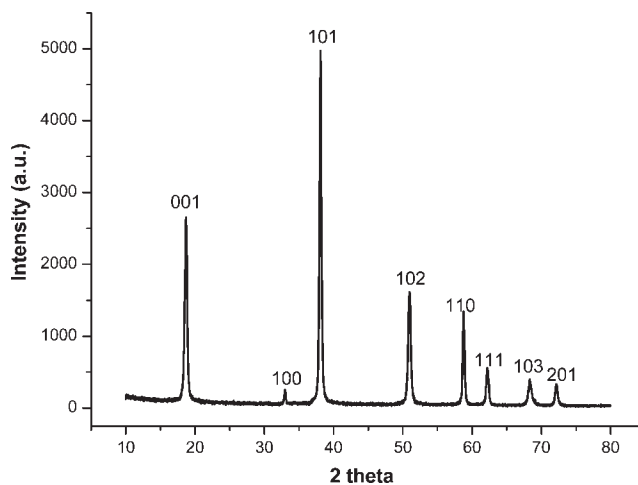


Figure 1 XPD pattern of MH nanocrystals with lamellar-like morphology.

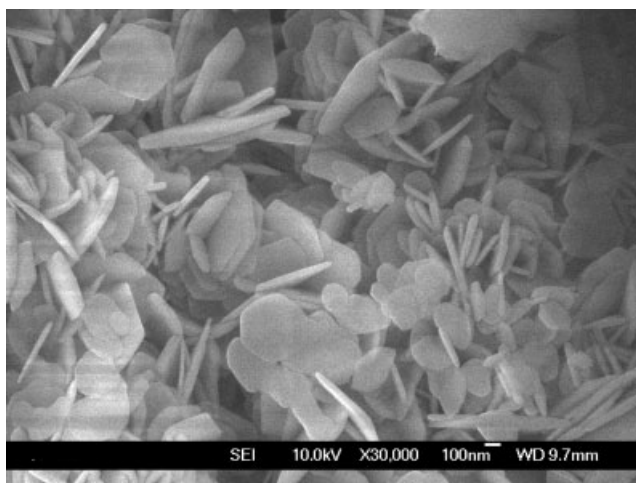


Figure 2 FESM micrograph of MH nanocrystals with lamellar-like morphology.

presumed to have monodispersed size range of about 350 nm in diameter and 50 nm in thickness.

Preparation of EVA/MH/MRP blends

The EVA samples were mixed as 40 g batch of EVA with the desired amounts of MH and MRP additives for 10 min at 130°C using a Rheomixer XSS-300. After mixing, the samples were hot-pressed into sheet of suitable thickness under 10 MPa for 5 min at 180°C. Each sample was then rapidly cooled to room temperature in air. Sheet size and thickness were dependent on the testing methods used in the present study.

Measurement of FR properties

LOI values were measured using a HC-2 type instrument (made in China) on the specimens of $120 \times 6.5 \times 4 \text{ mm}^3$ according to the standard oxygen index test ASTM D 2863-77. The UL-94 vertical burning tests were carried out using a CZF-1 type instrument (made in China) on the sheets $127 \times 12.7 \times 3 \text{ mm}^3$ according to the standard UL-94 test ASTM D 635-77. Stanton Redcroft Cone Calorimeter (made in England) tests were carried out on the samples of $100 \times 100 \times 3 \text{ mm}^3$ according to ISO 5660 standard procedures. Each specimen was wrapped in aluminum and exposed horizontally to an external heat flux of 35 kW/m^2 . The parameters of these flammability characterizations are time to ignition (TTI, s), average and peak heat release rate (av-HRR and pk-HRR, kW/m^2), average effective heat of combustion (av-EHC, MJ/kg), and mass loss rate (MLR). The experimental error of data from the cone calorimeter was about 10%.

Measurement of mechanical properties

The tensile strength and elongation at break were measured with an Instron Universal Tester (model 1185) at $25 \pm 2^\circ\text{C}$ with a crosshead speed of 25 mm/min. The dumbbell-shaped specimens were prepared according to ASTM D 412-87. In the measurements, five samples were usually analyzed to determine the average value to obtain reproducible results.

Characterization of MH nanocrystals

X-ray diffraction (XRD) analysis was carried out using a Philips X'Pert PRO SUPER apparatus (Nicolet Instrument, USA) with Cu K α ($\lambda = 1.5418 \text{ \AA}$) radiation at a scan rate of $0.0167^\circ/\text{s}$. FESEM (JSM-6700F, JEOL Lit, Japan) was used to characterize the morphology of the MH nanocrystals, and transmission electron microscope (TEM, HITACHI H-800) the final polymer formulations.

Thermogravimetric analysis

TGA was carried out in air using a STA409C thermogravimetric analyzer. In each case, $10 \pm 0.5 \text{ mg}$ sample was examined under an air flow rate of $6 \times 10^{-5} \text{ m}^3/\text{min}$ at temperature ranging from room temperature to 800°C.

Dynamic FTIR spectra

The dynamic FTIR spectra were recorded using a Nicolet MAGNA-IR 750 spectrometer equipped with a heating device and a temperature controller. The film samples of EVA/MH/MRP were placed in a ventilated oven kept at 400°C with temperature fluctuation of $\pm 2^\circ\text{C}$ for dynamically measuring the FTIR spectra *in situ* during the thermooxidative degradation. The choice of temperature point was based on the simultaneous TG-DTA experimental results, which showed that the maximum oxidation peak of pure EVA in the TGA curve appeared at about 400°C.

RESULTS AND DISCUSSION

FR and mechanical properties of the EVA/MH and EVA/MH MRP blends

The LOI and UL-94 test are widely used to evaluate FR properties of materials and to screen FR formulations. Table I lists the related LOI and UL-94 data obtained from different loading levels of MH lamellar-like MH nanoparticles and common micrometer grade MH, respectively. The data in Table I show that the LOI values of nanosized MH samples are higher than those of the common micrometer grade MH (1–5 μm) samples in all additive levels, espe-

TABLE I
Comparison of MH on Flammable and Mechanical Properties
of Two Kinds of EVA/MH Blends

MH filler level (phr)	Nanosized MH particles $50 \times 350 \text{ nm}^2$			Micrometer grade MH particles A 1–5 μm		
	TS (MPa)	LOI (%)	UL-94	TS (MPa)	LOI (%)	UL-94
0	17.3	18	–	17.3	18	–
80	10.1	26	Fail	9.5	25	Fail
100	10.4	37	Fail	8.3	29	Fail
120	11.6	42	Fail	7.0	36	Fail
150	17.2	46	V-2	6.7	39	V-2

cially for the high additive levels. In the low MH loading level of 80 phr, the LOI values of nanosized MH and common micrometer grade MH all increase rapidly from 18 of original EVA sample to 26 and 25, respectively. When the additive levels increase from 100 to 150 phr, the LOI values of the nanosized MH composites are 6–7 higher than those of the corresponding micrometer-sized MH composites. The above data indicate that MH nanoparticles preserve higher FR efficiency than that of common micrometer grade MH. The enhancement of FR property can be postulated the formation of compact oxide layer in the process of endothermic decomposition of the overlapped MH nanoparticles with lamellar-like morphological structure. This oxide layer, which is similar to the structure of ceramics, may insulate the polymer and to trap and oxidize soot precursors, and thus prevents the materials from burning.¹⁵

Although LOI test is widely used and generally considered reproducible for a given sample, it is important to note that criteria used in the LOI method often have little correlation with flammability performance with other laboratory test procedure, particularly the widely reported UL94 vertical burn ignition test.¹⁶ The results obtained from the UL94 test in Table I show that when the total loading level of MH increased to as high as 150

phr, it may yield only a V-2 classification, even the LOI exceeded over 47.

When the total loading of FR additives decreased to 100 phr, the LOI value can also increased greatly with little part of MH substituted by MRP, as shown in Table II. The LOI values of sample P₁ containing 1.0 phr MRP increased rapidly from 37 to 51, and then increased slowly to the maximum 60 as the loading of MRP increased from 1.0 to 5.0 phr for sample P₃. When the loading of MRP exceeded 8 phr, the LOI values decreased slowly to 53. This is because red phosphorus is essentially a flammable material, so with higher amounts of MRP, polymers become more flammable. Furthermore, the data in Table II also show that all samples P₁–P₈ with 1–8 phr of MRP reach the V-0 rating. That gives the positive evidence that the incorporation of 1–3 phr MRP to MH nanocomposites can effectively decrease the total loading level of MH and keep the V-0 rating of the EVA/MH blends because of the synergetic effect of MRP with MH.

In the context of mineral-filled composites, mechanical properties are inevitably concerned besides their flammable characteristics. As discussed before, high weight fraction of MH filler additive level in polymers can adversely affect some mechanical properties, and often decrease their tensile strength.¹⁷

TABLE II
Loading Level of MRP Additive on the Flammable and Mechanical Properties
of EVA/MH Nanocomposite Blends

Sample	Compound (phr)		Mechanical property		Flammability	
	MH ($50 \times 350 \text{ nm}^2$)	MRP	TS (MPa)	EB (%)	LOI (%)	UL94
P ₀	100	0	10.4	235	37	Fail
P ₁	99	1.0	11.3	180	51	V-0
P ₂	97	3.0	13.3	240	55	V-0
P ₃	95	5.0	14.0	270	60	V-0
P ₄	93	7.0	14.2	270	59	V-0
P ₅	92	8.0	13.7	230	59	V-0
P ₆	90	10.0	13.1	210	57	V-0
P ₇	88	12.0	13.5	190	55	V-0
P ₈	86	14.0	13.5	190	53	V-0

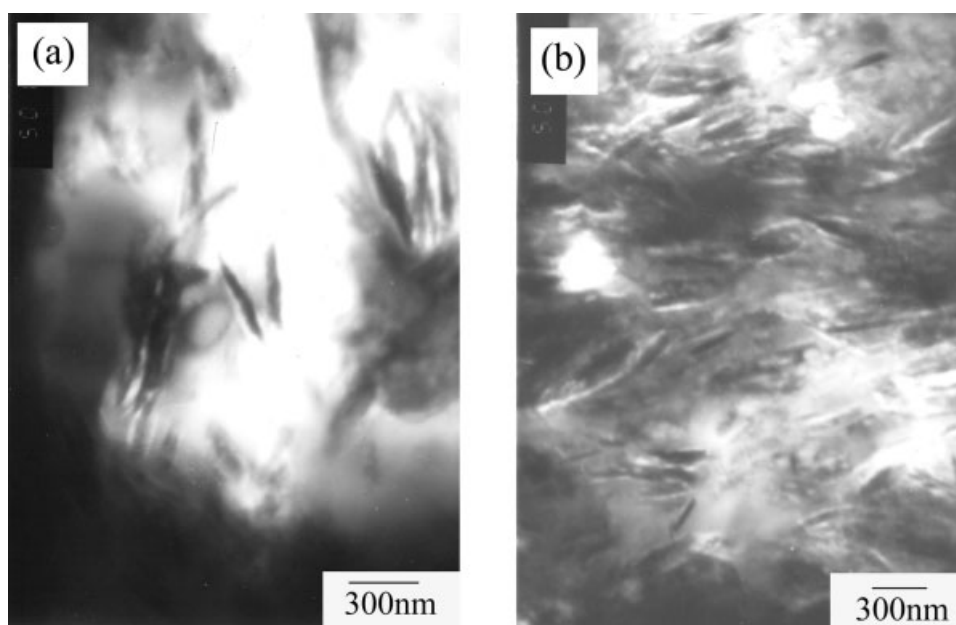


Figure 3 SEM micrographs of EVA/MH composites: (a) Sample P_0 (EVA/MH = 100/100), (b) Sample P_3 (EVA/MH/MRP = 100/95/5).

It can be seen from Table I that the values of TS for common micrometer grade MH decreased steadily from 9.7 to 7.1 MPa when additive level increased from 80 to 150 phr. In contrast, the values of TS for nanoparticles increased slightly from 10.4 to 11.0 MPa as the additive level increased from 80 to 120 phr. When the additive level of MH nanoparticles increased to 150 phr, TS value increased sharply from 11.0 to 17.0 MPa, which is approximate to 17.3 MPa for original EVA. The results testified that MH nanocomposites formation can enhance both fire retardancy and mechanical properties.

The data in Table II showed that micrograde MRP filler preserved some synergetic mechanical reinforcement effect with MH nanoparticles. The TS values increased from 10.4 MPa of samples P_0 to maximum 14.2 MPa of samples P_4 , and then decreased to 13.5 MPa of samples P_8 as the loading level of MRP increased from 1.0 to 14.0 phr. As the same as TS, the EB values of samples P_1 to P_8 increased from 180% to maximum 270% of sample P_3 , P_4 , and then decreased to 190% of sample P_8 . These data illustrated that a suitable amount of MRP can improve the mechanical property of EVA/MH nanocomposites. The synergetic mechanical reinforcement role of MRP may be the reason that a proper amount of micrometer particles can assist MH nanoparticles to disperse in polymeric blends, as reported in the literature.¹⁸

Therefore, it is clear from the preceding discussion that the formulation of sample P_3 with 5 phr MRP and 95 phr MH (total additive level 100 phr) is optimum for EVA/MH/MRP nanocomposite blends.

TEM measurement on the polymer formulations

The TEM images of sample P_0 with 100 phr MH and sample P_3 with 95 phr MH and 5 phr MRP are shown in Figure 3. Although the loading level was as high as 100 phr, it can be seen from the figures that fillers in both sample P_0 and sample P_3 were isolated each other by polymer materials. The obvious presence of filler agglomeration was not observed in both samples. In particular, the fillers tended to be overlapped with each other due to the large anisotropy of lamellar-like MH nanocrystals morphologic structure. Those isolated and overlapped nanocomposites may be the reason for their enhanced fire retardancy and mechanical properties.

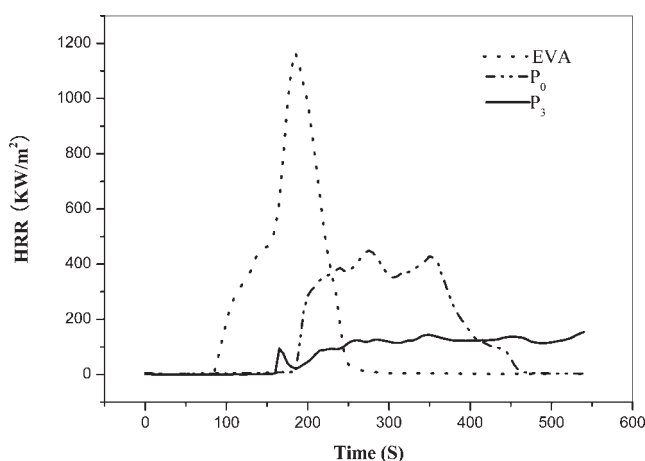


Figure 4 Dynamic curve of the HRR data versus burning time at a heat flux of 35 kW/m².

TABLE III
Data of Heat Release Rate and Mass Loss Rate Obtained from the Cone Calorimeter Tests

Sample	TTI (s)	pk-HRR (kW/m ²)	av-HRR (kW/m ²)	FPI (m ² s/k)	Figra (s ⁻¹)	av-EHC (MJ/kg)	av-MLR (g/s)
EVA	87	1165	439	0.07465	0.0054	32.8	0.134
P ₀	148	423	251	0.2458	0.0036	19.4	0.140
P ₃	176	148	72	0.9588	0.0022	18.6	0.031

Dynamic flammability characterization of the EVA/MH/MRP blends

As well known, the LOI and UL94 tests are useful tools to rank the flammability of a material in a small-scale fire, while CCT is regarded as one of the most effective bench-scale methods to measure many important parameters of a real fire. Although a CCT is in a small-scale, the obtained results have been found to correlate well with those obtained from a large-scale fire test and can be used to predict the combustion of materials in a real fire.^{19,20}

The HRR measured by CCT is a very important parameter as it expresses the intensity of a fire, which in turn determines other parameters, such as TTI, MLR, and EHC. A highly FR system normally shows a low av-HRR value. The pk-HRR value is used to express the intensity of a fire. The changes of HRR as a function of burning time for different samples are shown in Figure 1.

It can be found from Figure 4 that pure EVA burns very quickly after ignition. A very sharp HRR peak appeared at the range of 80–250 s, whereas sample P₀ with 50 phr MH showed a dramatic decline of the HRR curve and its combustion was prolonged to 450 s. The HRR of sample P₀ showed two separate peaks, which indicated the gradual burning of the specimen through the thickness after the initial charred layers were formed. It can be found that sample P₃ with 5 phr MRP preserved remarkable low HRR and its combustion did not cease even after 550 s interval, with a small peak appeared at the beginning of the curve. The reason can be postulated that MRP was an active additive in fire-retarded system. It quickly promoted the formation of charred layer through chemical process in the condensed phase, and greatly decreased the combustion speed by collaborating with MH, so the combustion speed only increased slowly under heat flux.

TTI is the time required for the entire surface of a sample to burn with a sustained flame, which can be measured from the onset of a HRR curve. FPI is defined as the ratio of TTI to pk-HRR, which is often used to predict whether a material can easily be developed drastic combustion after ignition. Therefore, the greater the FPI, the better is the fire resistance. FIGRA (fire growth rate) is defined as the ratio of pk-HRR/time to pk-HRR, which is also used to

predict fire safety of a material. In opposition to FPI, the lower the FIGRA, the slower the flame spread potential and the better the fire safety of the material. The data in Table III showed that, compared with sample P₀, the pk-HRR, av-HRR, av-MLR, and av-EHC for sample P₃ decreased dramatically. It also can be seen that sample P₃ had the greatest FPI value of 0.9588 and the lowest FIGRA value of 0.0022. The data indicated the fire-resistance performances of EVA/MH blends were enhanced by partly substituting MH with MRP.

The dynamic curves of mass versus time for the above three samples are shown in Figure 5. It can be seen that pure EVA lost its 99% mass at 250 s, because of its complete combustion. As expected, sample P₃ with 5 phr MRP lose mass more slowly than sample P₀. If we selected 40% mass loss as a reference point, it needs 160, 300 and 500 s for the samples of original EVA, P₀ and P₃, respectively.

Thermogravimetric behavior of the EVA/MH/MRP blends

The thermal degradation behaviors of the nanocomposites can be monitored by TGA in air. Figure 6(a) showed the thermogravimetric trace of these samples. The TGA data included the initial pyrolysis temperature (T_i) of the degradation, as measured by

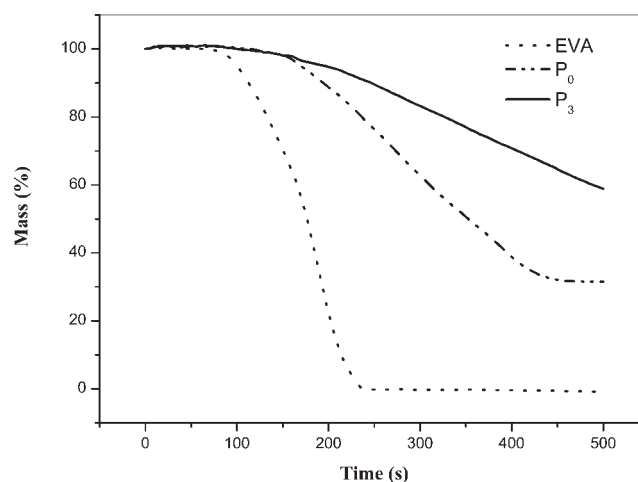


Figure 5 Dynamic curve of the mass loss versus burning time.

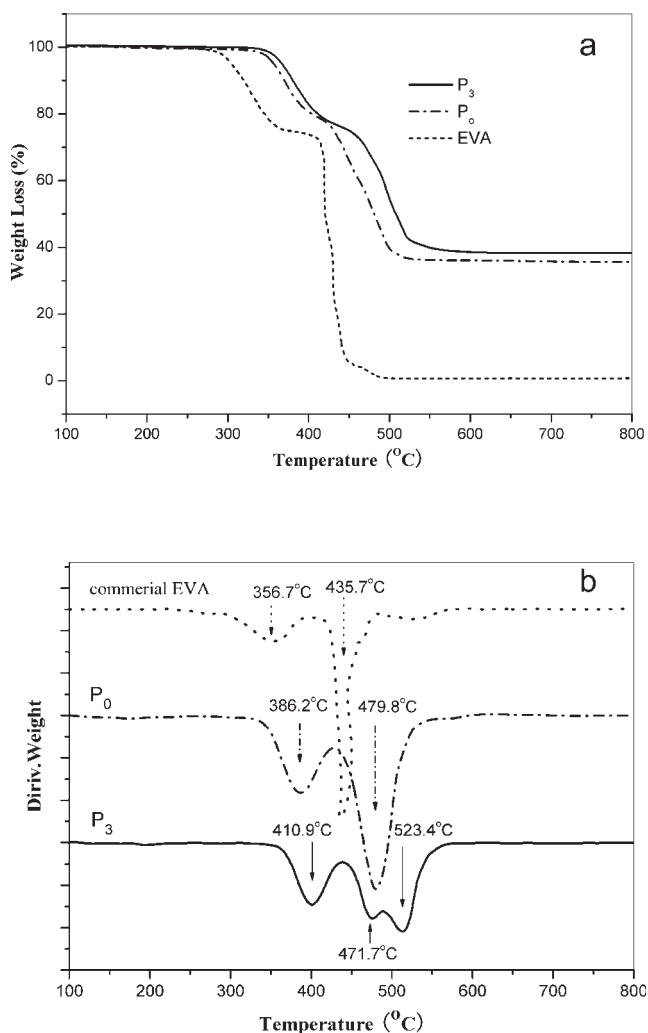


Figure 6 TG (a) and DTG (b) curves of samples P₃, P₀, and commercial EVA.

the temperature at which 1% of the mass had been lost, the maximum decomposition temperature (T_p), pyrolysis end temperature (T_e), weight fraction, and char yield.

It can be found from Table IV that the thermal stability of samples P₀ and P₃ are obviously superior to that of commercial EVA. For example, the T_i corresponding to the first DTG peaks for samples P₀ and P₃ increased from 226°C of commercial EVA to 290 and 349 °C, and the T_p increased from 438 to 470

and 490°C, respectively. The weight fraction for sample P₃ with MRP was 8% higher than that of sample P₀ without MRP after the heating temperature reached to 570 °C. The char yield of sample P₃ with 5 phr MRP was 16%, which is much higher than 6% of sample P₀ without MRP, as shown in Table IV. The char layer limited the production of flammable gases, thus decreased the exothermicity of pyrolysis reactions and inhibited the thermal conductivity of the burning materials, so that leveled up the flame retardancy of the polymeric composite.

Figure 6(b) showed the derivative thermograms (DTG), which gave the weight loss rates in the heating process. It can be seen that the EVA thermal degradation occurs in two steps. The first step was considered to involve dehydration of MH and the loss of acetic acid in temperature range 325–440°C, and the second step was due to the volatilization of the residual polymer in temperature range 420–560°C. It also can be seen in Figure 6(b) that the second peak of sample P₃ was broadened markedly, and composed of two overlapped peaks. That indicated that MRP in the blend must have some chemical reactions with polymer or changed the pyrolysis program more or less in the pyrolysis process. Those chemical reactions between MRP and EVA in the range 560–800°C promoted the formation of more stable carbonaceous layer containing P–O and P–C complexes, which could cover the burning surface of sample and inhibit oxygen from entering the flaming zone.

Dynamic FTIR spectra of the thermooxidative degradation of EVA/MH/MRP blend

The chemical reactions taken place between FRs and polymer molecules in thermal-oxidative degradation can be monitored by dynamic FTIR spectra. Figure 7 presented the dynamic FTIR spectra of the thermooxidative degradation of EVA/MH/MRP blend (sample P₃) at 400 °C. After 2 S' interval, MH decomposed rapidly and released almost all the hydration water, and the peak at 3686 cm⁻¹ assigned to OH which disappeared instantly. The intensities of peaks at 1284, 1265, 1080, and 880 cm⁻¹ (assigned to P–O–P, P–O–C, and PO₃ complex structures)

TABLE IV
TGA Data for EVA Nanocomposites^a

Sample	T_i (°C)	T_p (°C)	T_e (°C)	Weight fraction (%) (520°C)	Char yield ^b (%) (800°C)
Commercial EVA	226	438	485	7	0
P ₀	290	470	520	36	6
P ₃	349	490	570	44	16

^a Measured on a sample of 10 ± 0.5 mg and a heating rate of 10°C/min under a air flow of 30 mL/min.

^b Char yield: [weight (total) – weight (MgO)]/weight fraction of polymer.

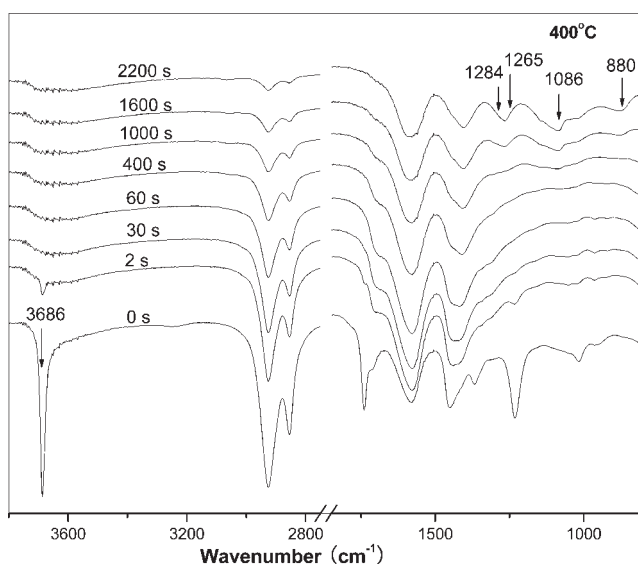


Figure 7 Dynamic FTIR spectra obtained from the thermo-oxidative degradation of sample P₃ in the condensed phase with different pyrolysis time at 400°C.

increased slowly with increasing thermal-oxidative degradation times, which showed that the MRP had to take some time to be predominantly oxidized to various phosphoric acid derivatives. These derivatives then reacted with EVA to form more stable char structures containing P—O—P and P—O—C complexes. These dynamic thermo-oxidative data gave positive evidence of the two-step FR mechanism, which is coincided with the DTG results shown in Figure 3(b). First, MH decomposed very quickly with the release of 30.1% hydration water in the 320–370°C temperature range. The endothermic decomposition reduced the temperature, and the released water steam diluted the combustion gas. Second, MRP promoted the formation of compact charred layers in the condensed phase in the 450–550°C temperature range after 1600 s' interval. In addition, little phosphorus monoxide (PO•) species produced from the combustion of MRP can quench active radicals produced by burning in gas phase.^{21,22} The combined two-step effects slowed down heat and mass transfer between the gas and condensed phase, and prevented the underlying polymeric substrate from further attack by heat flux in a flame.

CONCLUSIONS

Lamellar-like MH nanoparticles with 350 nm in diameter and 50 nm in thickness show better FR efficiency and reinforced mechanical property in EVA/MH blend than common micrometer grade MH in all loading levels. The values of LOI for nanosized

MH are 1–7 higher than those of the corresponding common micrometer grade MH. The values of TS for MH nanoparticles increase from 10.4 to 17.0 MPa as the additive levels increase from 80 to 150 phr. In contrast, the values of TS for common micrometer grade MH decrease steadily from 9.7 to 7.1 MPa. The LOI, UL-94, and CCT data reveal that MRP has a good FR synergistic effect with MH nanoparticles in the EVA/MH/MRP blends. MRP can increase the LOI value from 37 to 60 while keeping V-0 rating, which decreases the total amount of 150 phr MH to 100 phr MH. The optimum amount of MRP in the blend is 5 phr. Furthermore, 5–7 phr micrometer grade MRP assist MH nanoparticles to disperse in polymeric blends, and both the values of TS and EB increase evidently.

TGA and dynamic FTIR spectra show two-step FR mechanism. First, MH decomposed very quickly with the complete release of hydration water. Second, MRP promoted the formation of compact charred layers in the condensed phase.

The corresponding author thanks Professor Baojun Qu (University of Science and Technology of China) for his valuable guidance.

References

- Weil, E. D. In Proceedings of the 3rd Beijing International Symposium Flame Retardants and Flame Retarded Materials, Beijing, China, 1999, p 177.
- Xie, R. C.; Qu, B. J. *J Appl Polym Sci* 2001, 80, 1181.
- Xie, R. C.; Qu, B. J. *J Appl Polym Sci* 2001, 80, 1190.
- Lu, S. Y.; Hamerton, I. *Prog Polym Sci* 2002, 27, 1661.
- Sen, A. K.; Mukherjee, B.; Bhattacharya, A. S.; Sanghi, L. K.; De, P. P.; Bhowmick, K. *J Appl Polym Sci* 1991, 43, 1673.
- Wang, Z. Z.; Qu, B. J.; Fan, W. C.; Huang, P. *J Appl Polym Sci* 2002, 81, 206.
- Li, Z. Z.; Qu, B. J. *Polym Degrad Stab* 2003, 81, 401.
- Fu, M. Z.; Qu, B. J. *Polym Degrad Stab* 2004, 85, 633.
- Pukánszky, B.; Fekete, E. *Adv Polym Sci* 1999, 139, 109.
- Rothon, P. N. *Adv Polym Sci* 1999, 139, 67.
- Gilbert, M.; Sutherland, I.; Guest, A. *J Mater Sci* 2000, 35, 391.
- Lv, J. P.; Qiu, L. Z.; Qu, B. J. *Crystal Growth* 2004, 267, 676.
- Henrist, C.; Mathieu, J. P.; Vogels, C.; Rulmont, A.; Cloots, R. *J Crystal Growth* 2003, 249, 321.
- Lv, J. P.; Qiu, L. Z.; Qu, B. J. *Nanotechnol* 2004, 15, 1576.
- Qiu, L. Z.; Xie, R. C.; Ding, P.; Qu, B. J. *Compos Struct* 2003, 62, 391.
- Weil, E. D.; Hirschler, M. M.; Patel, N. G.; Said, M. M.; Shakir, S. *Fire Mater* 1992, 16, 159.
- Ulutun, S.; Gilbert, M. *J Mater Sci* 2000, 35, 2115.
- Brown, S. C.; David, M. L.; *Fire Retardant Compositions*, WO 00/66657 2000.
- Babrauskas, V.; Peacock, R. D. *Fire Safety J* 1992, 18, 255.
- Babrauskas, V. *Fire Mater* 1995, 19, 243.
- Zheng, X. X.; Wilkie, C. A. *Polym Degrad Stab* 2003, 81, 539.
- Wu, Q.; Lv, J. P.; Qu, B. J. *Polym Int* 2003, 52, 1326.